



HAL
open science

Martian Eolian Dust Probed by ChemCam

J. Lasue, A. Cousin, P.-y. Meslin, N. Mangold, R. Wiens, G. Berger, E. Dehouck, O. Forni, W. Goetz, O. Gasnault, et al.

► **To cite this version:**

J. Lasue, A. Cousin, P.-y. Meslin, N. Mangold, R. Wiens, et al.. Martian Eolian Dust Probed by ChemCam. *Geophysical Research Letters*, 2018, 45 (20), pp.10968–10977. 10.1029/2018GL079210 . hal-02349332

HAL Id: hal-02349332

<https://hal.science/hal-02349332>

Submitted on 10 May 2021

HAL is a multi-disciplinary open access archive for the deposit and dissemination of scientific research documents, whether they are published or not. The documents may come from teaching and research institutions in France or abroad, or from public or private research centers.

L'archive ouverte pluridisciplinaire **HAL**, est destinée au dépôt et à la diffusion de documents scientifiques de niveau recherche, publiés ou non, émanant des établissements d'enseignement et de recherche français ou étrangers, des laboratoires publics ou privés.

RESEARCH LETTER

10.1029/2018GL079210

Special Section:

Curiosity at the Bagnold Dunes, Gale crater: Advances in Martian eolian processes

Key Points:

- The martian eolian dust chemical composition is homogeneous at the submillimeter scale
- The dust composition is different from the Aeolis Palus soils and Bagnold sands with a larger content of FeO and TiO₂ and lower hydration
- Although dust may be a contributor to the amorphous component of soils, its composition indicates that the two materials are not equivalent

Supporting Information:

- Supporting Information S1
- Data Set S1

Correspondence to:

J. Lasue,
jlasue@irap.omp.eu

Citation:

Lasue, J., Cousin, A., Meslin, P.-Y., Mangold, N., Wiens, R. C., Berger, G., et al. (2018). Martian eolian dust probed by ChemCam. *Geophysical Research Letters*, 45, 10,968–10,977. <https://doi.org/10.1029/2018GL079210>

Received 13 JUN 2018

Accepted 26 SEP 2018

Accepted article online 10 OCT 2018

Published online 23 OCT 2018

Martian Eolian Dust Probed by ChemCam

J. Lasue¹ , A. Cousin¹ , P.-Y. Meslin¹ , N. Mangold² , R. C. Wiens³ , G. Berger¹ , E. Dehouck⁴ , O. Forni¹ , W. Goetz⁵ , O. Gasnault¹ , W. Rapin⁶ , S. Schroeder⁷ , A. Ollila³ , J. Johnson⁸ , S. Le Mouélic² , S. Maurice¹ , R. Anderson⁹ , D. Blaney¹⁰ , B. Clark¹¹ , S. M. Clegg¹² , C. d'Uston¹, C. Fabre¹³, N. Lanza³ , M. B. Madsen¹⁴ , J. Martin-Torres^{15,16}, N. Melikechi¹⁷ , H. Newsom¹⁸ , V. Sautter¹⁹ , and M. P. Zorzano^{15,20} 

¹IRAP, Université de Toulouse, CNES, CNRS, UPS, Toulouse, France, ²LPGN, CNRS UMR 6112, Université de Nantes, Nantes, France, ³ISR, MS D466, Los Alamos National Laboratory, Los Alamos, NM, USA, ⁴Université de Lyon, UCBL, ENSL, CNRS, LGL-TPE, Villeurbanne, France, ⁵Max-Planck-Institut für Sonnensystemforschung, Göttingen, Germany, ⁶California Institute of Technology, Pasadena, CA, USA, ⁷German Aerospace Center (DLR), Institut für Optische Sensorsysteme, Berlin-Adlershof, Germany, ⁸Johns Hopkins University APL, Laurel, MD, USA, ⁹USGS, Flagstaff, AZ, USA, ¹⁰NASA JPL, Pasadena, CA, USA, ¹¹Space Science Institute, Boulder, CO, USA, ¹²C-PCS, MS J565, Los Alamos National Laboratory, Los Alamos, NM, USA, ¹³GeoRessources, Lorraine University, CNRS, Vandoeuvre, France, ¹⁴Niels Bohr Institute, University of Copenhagen, Copenhagen, Denmark, ¹⁵DST, Luleå University of Technology, Luleå, Sweden, ¹⁶Instituto Andaluz de Ciencias de la Tierra (UGR-CSIC), Granada, Spain, ¹⁷University of Massachusetts Lowell, Lowell, MA, USA, ¹⁸University of New Mexico, Albuquerque, NM, USA, ¹⁹IMPMC, Muséum d'Histoire Naturelle, Paris, France, ²⁰Centro de Astrobiología (INTA-CSIC), Torrejón de Ardoz, Spain

Abstract The ubiquitous eolian dust on Mars plays important roles in the current sedimentary and atmospheric processes of the planet. The ChemCam instrument retrieves a consistent eolian dust composition at the submillimeter scale from every first laser shot on Mars targets. Its composition presents significant differences with the Aeolis Palus soils and the Bagnold dunes as it contains lower CaO and higher SiO₂. The dust FeO and TiO₂ contents are also higher, probably associated with nanophase oxide components. The dust spectra show the presence of volatile elements (S and Cl), and the hydrogen content is similar to Bagnold sands but lower than Aeolis Palus soils. Consequently, the dust may be a contributor to the amorphous component of soils, but differences in composition indicate that the two materials are not equivalent.

Plain Language Summary Eolian dust on Mars is very fine dust that covers the entire surface of the planet, gives it its typical red hue, and is mobilized by wind. It plays a significant role in the current rock cycle of the planet and for the temperature of the atmosphere. ChemCam uses a series of pulsed laser shots to analyze the chemical composition of target materials. Each first laser shot by ChemCam gives the composition of the deposited dust. These measurements have been constant over the duration of the Mars Science Laboratory mission. The dust is homogeneous at the millimeter scale (approximately the size of the ChemCam analysis spot). Compared to local soils and sands at Gale crater, the dust contains higher levels of iron and titanium, associated with volatile elements like hydrogen, sulfur, and chlorine. We infer from this difference that the dust does not entirely originate locally and may be part of a separate global cycle.

1. Introduction

1.1. Eolian Dust on Mars

The study of fine dust aerosols on Mars is of prime importance to understanding eolian sedimentary and planetary atmospheric processes. Dust particles absorb solar radiation in the ultraviolet (UV) and visible wavelengths while emitting energy in the infrared (IR) and are therefore a driver of the atmosphere's thermal structure (e.g., Kleinböhl et al., 2009; McCleese et al., 2007).

The typical size distribution of the particles that constitute the solid aerosols transported by wind was first determined from the infrared spectra obtained by Mariner 9 during the 1971–1972 dust storm to be between 1 and 10 μm in radius following a power law with a –4 exponent (Toon et al., 1977). This distribution gives an average effective particle radius of 2.7 μm. Later studies using the Viking opacity measurements and combined measurements from several Mars missions (including opacity and infrared measurements) refined this

estimate to the range 1.5–2 μm under usual conditions, when a dust storm is not present (Clancy et al., 1995; Lemmon et al., 2004; Pollack et al., 1995; Tomasko et al., 1999; Wolff et al., 2006). More recent analysis of the Viking limb measurements at the edge of Mars' disk indicates a bimodal size distribution of the dust aerosol with the smallest part of the size distribution peaking at an effective radius around 0.2 μm and the average effective radius remaining consistently around 2 μm (Montmessin, 2002). Observed changes in the spectral slope in infrared data are consistent with a mean particle size of aerosols varying with time between 1 and 2 μm based on seasonal variations of albedo using OMEGA data (Vincendon et al., 2009). While those dust particles are quite small in size, they appear to readily cohere and form larger aggregates after deposition, measuring from ≈ 100 μm to several millimeters in size as observed on Mars Exploration Rover (MER) missions (Vaughan et al., 2010).

Infrared observations from orbit have been used to derive the mineralogical composition of the upper dust layer of the planet. Early observations from Viking orbiters suggest that the dust is mostly a complex assemblage of particles composed of igneous primary silicates minerals and weathering products, such as iron oxides and possible clay minerals (Toon et al., 1977). Anhydrous amorphous palagonites (a possible precursor of smectite produced by weathering of mafic glass) have been shown to provide a better fit to the infrared observations (Clancy et al., 1995). Analysis of the Thermal Emission Spectrometer observations suggests that framework alumino-silicates (feldspar with possible contribution of zeolites) dominate the dust mineralogy, with pyroxene, olivine, amorphous material (poorly crystalline silicates and nanophase oxides), (titano-)magnetite, and hematite as lesser amounts (Hamilton et al., 2005; Madsen et al., 2009; Ruff, 2004), although the relative abundance of these minerals may vary with altitude and atmospheric dust loading.

Chemical observations of the eolian dust were performed by previous Mars missions. Dust particles from the martian atmosphere were captured by the MERs magnets and analyzed by Mössbauer spectroscopy and the Alpha Particle X-ray Spectrometer (APXS). The spectra taken differentiate two populations of dust: one strongly magnetic and dark brown to black and one weakly magnetic and bright red in color. The weakly magnetic subgroup is enriched in Si, S, Ca, and K, while the strongly magnetic particles are dominated by Fe, Ti, and Cr (Madsen et al., 2009; Ming et al., 2008). This magnetic fraction of the dust contains magnetite, olivine, and some ferric oxide indicating limited alteration (Goetz et al., 2005). The chemical composition of bright undisturbed soils, interpreted as dust deposits was also measured with APXS (Gellert et al., 2006; Yen et al., 2005). Similar results are obtained for the mineralogy of the finest fractions of soils assumed to be representative of bright eolian dust deposits (Morris et al., 2006). Mars Science Laboratory (MSL) has shown that the finest fraction (<150 μm) of the Rocknest eolian ripple at Gale crater is very similar in composition to the soils measured at Meridiani Planum and Gusev crater, implying globally similar basaltic soils (Blake et al., 2013). Thirty to forty-five percent of the soil is X-ray amorphous, and this fraction contains the volatile elements H, S, P, and Cl measured in soils (Leshin et al., 2013; Meslin et al., 2013). Finally, the APXS on-board MSL analyzed air fall dust on the titanium observation tray of the rover and determined its chemical composition and associated enrichments in S, Cl, and Fe consistent with previous Viking lander and MER studies (Arvidson et al., 1989; Berger et al., 2016; Clark et al., 1982; Gellert et al., 2006; Yen et al., 2005). The dust chemical composition is discussed in detail in section 3. Details on Mössbauer spectroscopy, APXS, and CheMin can be found in Klingelhöfer et al. (2003), Rieder et al. (2003), Campbell et al. (2012), and Blake et al. (2012).

The ChemCam instrument on-board MSL provides a new methodology to constrain the chemical composition of this ubiquitous material.

1.2. The ChemCam LIBS Instrument

ChemCam is a Laser-Induced Breakdown Spectroscopy (LIBS) instrument on-board the NASA MSL rover that has been exploring Gale crater, Mars, since 2012. A nanosecond pulsed infrared laser is focused to the target of interest and briefly heats it to about 10000 K generating a plasma of electrons, ions, and atoms, the light of which is collected by a small telescope and analyzed by spectrometry (Maurice et al., 2012; Wiens et al., 2012). Thanks to its ability to analyze the composition of geological targets at a distance from the rover and without initial preparation, ChemCam is an ideal survey instrument to detect changes in composition in the vicinity of the rover. The technique can analyze the major rock-forming elements and is very sensitive to elements with low excitation energies such as the alkalis. Over its 5 years of exploration at Gale, ChemCam has acquired more than 500,000 spectra and analyzed around 13,000 different locations.

The spot size of the LIBS analysis ranges from ≈ 350 μm when the target is 1.2 m away to ≈ 550 μm when the target is 7 m away. For every target, a single shot removes a few tens of nanograms of material or about 1 μm

in depth. The first few laser shots can be used to clean the surface of a rock from weathering rind or dust deposited on its surface (Lanza et al., 2015). The instrument can also be used in passive mode, which provides useful reflectance spectra from 400 to 840 nm to assess the mineral composition of rocks (Johnson et al., 2015). The LIBS instrument is complemented by a Remote Micro-Imager (Maurice et al., 2012). This imaging capability ranges from 1.2 m to infinity, with a pixel scale of 19.6 μrad . In practice, the Remote Micro-Imager provides a resolution of about 80 μm at 2 m and 400 μm at 10 m (Le Mouélic et al., 2015).

ChemCam data acquisition is designed such that each spectrum generated by a single laser pulse can be recorded and analyzed independently. This feature has provided one key result: the chemical composition information carried by the first laser pulses onto a typical Mars target, and often up to the first five, is very reproducible and does not depend on the substrate (Melikechi et al., 2014; Mezzacappa et al., 2016). Such spectra are systematically removed from the quantification analysis of the rock targets (Wiens et al., 2013).

Due to its versatility, ChemCam is ideally suited to carry out a statistical survey of martian target composition at the submillimeter scale. The following work compiles the ChemCam first shots taken on calibration targets and martian targets over the first 4 years of the mission to refine the composition of the eolian fine dust detected by ChemCam.

2. Martian Eolian Dust Deposition and Composition

2.1. Eolian Dust Deposition

Fine dust aerosols are mobilized by eolian processes on the surface of Mars constantly depositing on Mars rovers and sometimes removed by the action of wind (Vaughan et al., 2010). A number of observations made by MSL indicate that eolian dust is mobilized at Gale and constantly deposits on the rover and its surroundings. They include

1. a change in the dust opacity measurements baseline with time using the UV sensors of the REMS meteorological station (supporting information Figure S1; Gómez-Elvira et al., 2012).
2. ChemCam passive spectroscopy has also been used to assess the variations in dust cover from the rover paint target located among the ChemCam Calibration Targets (CCCT). The passive spectroscopy documents reddening of the rover paint CCCT with time that indicates deposition of the dust particles on its surface (supporting information Figure S2; Johnson et al., 2015).
3. Dust particle movements are detected on the ChemCam calibration targets probably due to wind (supporting information Figure S3) and definitely during ChemCam active laser calibration sequences (supporting information Figure S4).

These observations are fully described in the supporting information.

Due to its mobility and continuous deposition, we analyze dust mostly from airborne origin which should consist of a typical grain size distribution around 1–2 μm as described in section 1.1. As such, this dust composition likely reflects that of the atmospheric and easily mobilized portion of regional and/or global martian dust cover.

2.2. Qualitative Assessment From Calibration Targets

ChemCam's first spectrum on the CCCT records the composition of dust. Most CCCTs have compositions simulating those of Mars soils and rocks (Fabre et al., 2011; Vaniman et al., 2012), making it difficult to disentangle the dust signal. One calibration target is made of pure graphite that yields much fewer emission lines, with low intensities, and can thus be used to qualitatively assess the composition of its dust cover. Graphite spectral lines would overlap with any C emission line from organics or carbonates if they were present in the fine dust. Thermal infrared spectra suggest the presence of small concentrations (2 to 5 wt.%) of carbonates in the dust (Bandfield et al., 2003); however, any such contribution would be minor and therefore difficult to detect with ChemCam (Beck et al., 2017; Ollila et al., 2011, 2013).

The first spectrum clearly presents all the major elements (Fe, Si, Mg, Al, Ca, Ti, Na, K, and O) that are absent from a clean C spectrum. Hydrogen and other volatiles are detected based on their emission lines indicating that the deposited dust material is hydrated and/or hydroxylated. Due to the thinness of the dust cover and matrix effects associated with the large carbon content, it is challenging to quantify the spectra thus obtained. We therefore do not discuss the graphite calibration target dust results further in this work.

2.3. Eolian Dust Composition

2.3.1. Method

Since the martian targets are covered with a thicker layer of dust than the calibration targets, we prefer to consider a statistical average of this dust spectrum for compositional quantification. We make use of the spectra available over the first 1,500 sols, giving us reasonable statistics. A part of the data set (between sols 805 and 980) cannot be used, as, during that time, the continuous laser diode used for LIBS focalization was not operating and focusing of the laser was determined by the intensity of the LIBS signal, implying that every first shot on the target was out of focus. A new focusing procedure based on imaging was introduced after sol 980, and we include in our analysis the first-shot data taken after this date. We have removed data taken on nearly dust-free surfaces, that is, the surfaces where the Dust Removal Tool or the drill was applied, the surfaces that were covered with subsurface material (the tailings and dump piles), and the surfaces where ChemCam active analysis is repeatedly applied at the exact same location: analysis of the CCCT, depth profiles, and z-stacks.

After this selection of targets, 8,466 spectra of first shots can be used to generate a median dust spectrum. Each spectrum has been denoised, corrected for the dark (nonlaser reflectance spectrum), corrected for the continuum emission, wavelength calibrated, and corrected for the instrument response (details in the data processing and analysis are described in Clegg et al., 2017, and Wiens et al., 2013). These first shots spectra major oxides compositions can be used to determine a first quantification of the elements contained in the eolian dust using the calibration database from ChemCam for major-element composition (Clegg et al., 2017).

The composition thus calculated is uncorrelated with the underlying targets composition, demonstrating the independence of the dust composition with respect to the substrate (see supporting information Figure S5). A 3-sigma discrimination threshold is further applied to remove potential first shots outliers or matrix effects from the substrate originating from relatively dust-free targets. The density distribution of the oxides composition is obtained as a smooth fitting function of their histogram, normalized to an integral of 1. This allows to compare distribution of compositional values, which will be discussed in section 3.1.

2.3.2. Results

Based on the procedure described above, a median spectrum for the first shots of ChemCam can be generated and its major oxides composition quantified. The median dust spectrum is to first order similar to the average spectrum of soils at Gale (Aeolis Palus soils) and the average spectrum of Bagnold dunes (Cousin et al., 2015, 2017). This is illustrated in supporting information Figure S6. Figure 1 and Table 1 give the results of the quantification procedure for this spectrum of eolian dust. The median absolute deviation (a robust statistical estimator of the standard deviation) for each quantified oxide is low, indicating that the variation in composition is relatively limited. The dust composition derived from first shots on soils and rocks is practically identical, showing that the first micrometers analyzed by ChemCam on rocks do not correspond to alteration rinds but to eolian dust. The dust appears homogeneous at the 350- μm scale of the ChemCam analysis spot. This likely indicates efficient eolian mixing of dust grains originating from different sources. Alternatively, it could indicate that the majority of the eolian dust grains originate from a single location on Mars with a specific composition as suggested by Ojha et al. (2018).

We can then compare the values obtained with dust measurements made by APXS on the MSL O-tray (Berger et al., 2014, 2016), the average Mars soils compositions as measured by ChemCam (Cousin et al., 2015, 2017; Meslin et al., 2013) and APXS at Gale (O'Connell-Cooper et al., 2017), and the average Mars soil composition from the MER rovers (Taylor & McLennan, 2009). The APXS measurements (for MER and MSL), which do not quantify H_2O , have all been normalized to a 2 wt.% H_2O content similar to the value measured by the Sample Analysis at Mars (SAM) instrument on-board MSL at Rocknest (Leshin et al., 2013; Sutter et al., 2017). Similar to ChemCam, APXS performed a chemical analysis of the dust by measuring the accumulation of dust on the O-tray (Berger et al., 2014, 2016). The APXS dust results are within 1σ of the ones obtained by ChemCam as shown in Table 1, except for the Na_2O and the K_2O contents, which appear lower for the ChemCam measurement, and the SiO_2 which appears enriched. We suspect that LIBS analysis of unconsolidated materials may lower the apparent alkali content of the targets, but this requires further study. The APXS dust analysis indicated compositions similar to the fine-grained fraction (<150 microns) of the Rocknest fines soil sample measured on the O-tray. A slight enhancement in SO_3 and Cl content is observed in the O-tray dust analysis compared to the average martian soil of Taylor & McLennan, (2009; 8.3 and 1.1 wt% instead of 6.2 and 0.7 wt%, respectively; Berger et al., 2016).

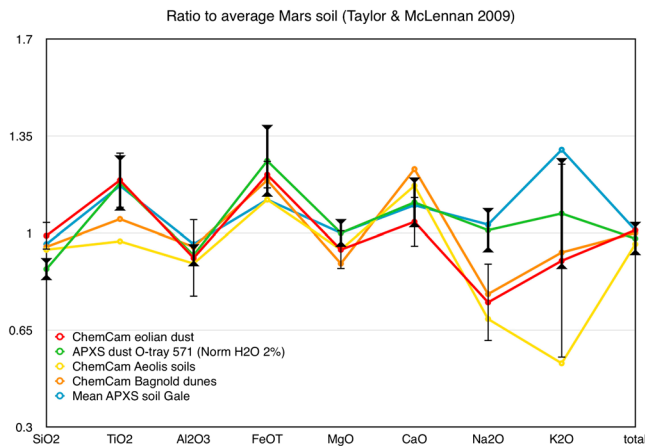


Figure 1. Comparison between the ChemCam eolian dust composition (red), the APXS dust composition from O-tray measurements (green, Berger et al., 2016), the Bagnold dunes sands measured by ChemCam (orange, Cousin et al., 2017) and the Mars soils measured at Gale by ChemCam (yellow, Cousin et al., 2017), and APXS (blue, O’Connell-Cooper et al., 2017) normalized to the average martian soils from Taylor and McLennan (2009). For clarity, only the error bars of the ChemCam (horizontal terminations) and APXS (triangle terminations) eolian dust compositions are indicated. Table 1 gives the values for the other curves. APXS = Alpha Particle X-ray Spectrometer.

The eolian dust composition inferred from ChemCam and APXS follows the same trends as compared to the average martian soil of Taylor and McLennan (2009). Alkalis are variable, while minor elements (like Ba, Sr, Rb, and Li) are detected at similar levels to previous ChemCam soil analyses (Cousin et al., 2017). Comparing the dust spectrum to the ones of typical ChemCam soils, Mn and Cr appear to have larger peak areas. The reported major oxide compositions present low totals, which we assume is dominated by the S, Cl, P, and H volatile elements (see section 6 in Clegg et al., 2017). S and Cl peaks are detected in the ChemCam dust spectrum, even though those elements are difficult to detect with LIBS. This agrees with the enrichment of S and Cl in the dust determined by APXS on MSL.

Finally, every ChemCam first shot presents a strong hydrogen signal, indicating that this fine dust contains some hydrated phases. The minor elements peaks comparison in the ChemCam spectra is detailed in supporting information Figure S7.

3. Discussion

3.1. Comparison to the Local Soils and Sand at Gale

Dust is omnipresent at Gale and contaminates the local soils and sand. At the same time, continued mechanical breakdown of the soils contributes to the eolian dust. It is therefore of interest to compare both sets of data.

Over the first 250 sols of the mission, the ChemCam instrument identified several soil components: a fine-grained mafic type with significant content of hydrated amorphous material and some coarse-grained types. The coarse-grained soil material can be separated into three groups depending on their composition: The first group is similar to the fine-grained soils; the second group is a locally derived, coarse-grained felsic type; and the third group presents a specific basaltic composition enriched in Cr and Mn (Cousin et al., 2015; Meslin et al., 2013). These groups are interpreted as a mechanical mixing between

Table 1
Comparison of Fine Dust and Soils Composition on Mars

	SiO ₂	TiO ₂	Al ₂ O ₃	FeOT	MgO	CaO	Na ₂ O	K ₂ O	Total
ChemCam eolian dust (sols 1 – 1,500)	44.00	1.05	8.70	19.80	7.70	6.50	2.01	0.39	90.15
median absolute deviation	2.40	0.09	1.33	0.74	0.59	0.59	0.37	0.15	—
Aeolis Palus soils ^a	42.00	0.86	8.50	18.40	7.70	7.30	1.86	0.23	86.85
median absolute deviation	1.50	0.10	0.74	1.30	0.74	0.40	0.23	0.09	—
Bagnold dunes ^a	42.15	0.93	9.00	19.50	7.30	7.70	2.10	0.40	89.08
median absolute deviation	1.10	0.03	0.60	0.44	0.50	0.20	0.10	0.06	—
The following values are normalized to H ₂ O = 2 wt.%.									
APXS dust O-tray 571 ^b	38.53	1.04	8.74	20.59	8.15	6.90	2.70	0.46	87.10
error	1.67	0.09	0.38	2.16	0.37	0.59	0.22	0.09	—
APXS disturbed soil Sourdough ^b	42.16	1.08	9.23	19.70	8.11	7.03	2.73	0.44	90.46
error	0.49	0.03	0.19	0.29	0.17	0.08	0.14	0.02	—
APXS Average Gale soil ^c	42.61	1.03	9.19	18.36	8.19	6.88	2.75	0.56	89.56
error	0.51	0.05	0.21	0.23	0.22	0.08	0.14	0.03	—
Average martian soil ^d	44.52	0.88	9.52	16.40	8.19	6.25	2.68	0.43	88.86
Rocknest am. comp. 35 wt.% ^e	34.58	2.12	5.45	23.27	4.05	4.45	3.38	1.39	—

Note. APXS = Alpha Particle X-ray Spectrometer.

^aCousin et al. (2015); ^bDisturbed soil target Sourdough, Sol 673, Berger et al. (2016); ^cO’Connell-Cooper et al. (2017); ^dTaylor and McLennan (2009); and ^eRocknest amorphous component quantified as a 35 wt.% contribution in Achilles et al. (2017). These values are not normalized and correspond to upper limits. They would require to be normalized to H₂O = 5 to 9 wt.% to be comparable to ChemCam data.

a globally representative finer soil component and locally derived sources from rocks (Sautter et al., 2014; Stolper et al., 2013). We define the Aeolis Palus soils to correspond to the fine-grained fraction of any loose, unconsolidated materials that can be distinguished from cohesive rocks at Gale, following Cousin et al. (2017). As compared to the average martian soils, the Aeolis Palus soils have low SiO_2 (42 wt.%) and low *total oxide values* (86.9 wt.%) with around 13 wt.% of oxides unaccounted for as shown in Table 1. This suggests a greater abundance of elements that are not easily detected or quantified by LIBS (H, C, N, P, S, Cl, and F).

ChemCam also analyzed the Bagnold dunes, an active dune field at the foot of Aeolis Mons in Gale. Bagnold sediments range from very fine, $\approx 45 \mu\text{m}$, to medium sized, $\approx 500 \mu\text{m}$ (Cousin et al., 2017; Ehlmann et al., 2017). Their composition determined by ChemCam is well within 1σ of Aeolis Palus soils but appears depleted in the alkali and volatile-rich amorphous component or fine-grained particles presents in soils (see also, Gabriel et al., 2018). A higher content in elements such as Fe or Mn is probably associated with a larger content in olivine as compared to soils (Cousin et al., 2017).

The dust from the ChemCam's first shots appears to be within 1σ of Aeolis Palus soils and Bagnold dunes compositions, as shown in Table 1 and Figure 1. Figure 2 compares the density distribution of compositions between the dust, Aeolis Palus soils, and Bagnold dunes in SiO_2 , FeO, CaO, and the hydrogen content as estimated from an independent component analysis. ChemCam is sensitive to hydrogen (Rapin et al., 2017; Schröder et al., 2015), and independent component analysis can be used to extract spectral information related to a single element, as its score correlates with the emission of atoms present in the plasma (Forni et al., 2013). The vertical red lines indicate values of the average Mars soils as derived by Taylor and McLennan (2009). From the distributions of those elements and the values reported in Table 1, one notices $> 1\sigma$ differences between the dust, the Aeolis Palus soils, and Bagnold dunes. The dust composition appears lower in CaO, and higher in SiO_2 and FeO than the Aeolis Palus soils. The dust content in TiO_2 , MnO, and Cr is also higher as shown from peak height comparison in supporting information Figure S7. The elevated iron content of the dust may be linked to the presence of different phases such as olivine or nanocrystalline ferric oxides as detected earlier by the MER rovers (Goetz et al., 2005). Finally, one can notice that the composition of Aeolis Palus soils is not intermediate between Bagnold dunes and eolian dust and hence cannot be solely described as a mixture between these two end-members.

The low SiO_2 and anhydrous total values in soils may be attributed to the presence of an amorphous component that is observed as a soil component (Cousin et al., 2015; Meslin et al., 2013) by ChemCam. This component is detected in the Rocknest soil by CheMin and quantified by CheMin and APXS at levels of 20 to 50 wt.% (Achilles et al., 2017; Bish et al., 2013; Blake et al., 2013). From mass balance calculations, this component is low in Si ($\text{SiO}_2 = 25.6\text{--}38.7$ wt.%) while enriched in S, Cl, and possibly P (with values of $\text{SO}_3 = 14.7\text{--}17.2$ wt.%, $\text{Cl} = 2.0$ wt.%, and $\text{P}_2\text{O}_5 = 3.1$ wt.%; Achilles et al., 2017; Blake et al., 2013; Dehouck et al., 2014). The SAM experiment results also predicted 5 to 9 wt.% of H_2O for the amorphous component (Leshin et al., 2013). Individual phases proposed to be present in the amorphous component include: volcanic (or impact) glass, hisingerite (or silica + ferrihydrite), amorphous sulfates, and nanophase ferric oxides (Bish et al., 2013; Dehouck et al., 2014). Their calculated compositional ranges shown in Table 1 are not consistent with the eolian dust composition, indicating that the amorphous phase component of the soils cannot be explained by a simple eolian dust contribution. While eolian dust may be a contributor to the soils amorphous component, the latter appears to contain a greater proportion of altered phases, probably of local origin, as not accounted for by eolian dust.

The dust spectra also show the presence of volatile elements (S, Cl, and H; see supporting information Figure S6). As illustrated in Figure 2, the hydrogen content of dust is similar to the Bagnold dunes sands, but lower than the typical Aeolis Palus soils. This indicates that eolian dust may contribute to the soils hydration but cannot explain it entirely. Long-term analysis of the soils over the mission and several experiments comparing daytime and nighttime soil and dust analyses have not revealed significant exchange of water vapor between the regolith and the atmosphere from ChemCam data (Meslin et al., 2013; Schröder et al., 2015). However, the D/H ratio of the fines (measured by SAM) is similar to the current atmospheric value (Ehlmann et al., 2017; Leshin et al., 2013), indicating that alteration products present in the Rocknest soil likely resulted from weathering under hydrous conditions similar to those prevalent today. ChemCam showed that the fine fraction of Rocknest soils had the same chemical composition as the average Aeolis Palus soils (Cousin et al., 2015; Meslin et al., 2013). Also, Rocknest may be considered to be typical of basaltic Martian soils based on a striking similarity between their measured and estimated mineralogies (Achilles et al., 2017; Bish et al., 2013; Blake

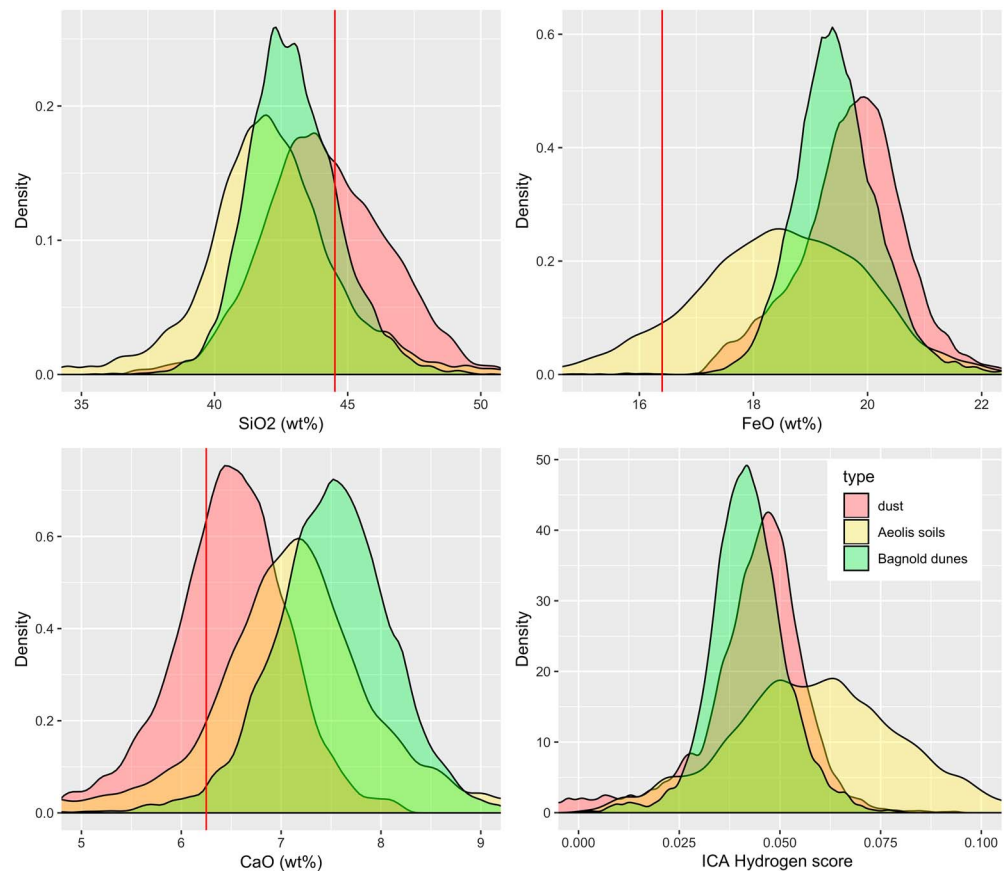


Figure 2. Comparison between the composition density distributions for eolian dust (red) as calculated from the first shots analysis, the Aeolis Palus soils (yellow), and the Bagnold dunes (green) at Gale. Top left corresponds to SiO_2 , top right to FeO , bottom left to CaO , and bottom right to the hydrogen signal as extracted from the ICA analysis. The vertical red lines indicate values of the average Mars soils (Taylor & McLennan, 2009). ICA = independent component analysis.

et al., 2013). Therefore, the hydrogen signature in soils and in the eolian dust may originate from the current hydration of their respective phases following different processes.

3.2. Comparison to Previous Dust Measurements

The MERs used permanent magnets to collect the magnetic fraction of atmospheric dust for investigation (Madsen et al., 2003). Those magnets are of different strengths, and the images taken by the cameras differentiate two populations of dust: one that is strongly magnetic and dark brown to black, and one that is weakly magnetic and bright red in color. The weakly magnetic subgroup is enriched in the elements Si, S, Ca, and K, while the particles in the strongly magnetic one are dominated by the elements Fe, Ti, and Cr (Madsen et al., 2009). The magnetic fraction deposited on the magnets was shown by Mössbauer to contain magnetite, pyroxene, and olivine, indicating a basaltic origin for the dust. The presence of olivine is an indicator that aqueous alteration did not play a dominant role in the formation processes of the atmospheric dust (Goetz et al., 2005) or that the alteration was incomplete. The dust also contains ferric oxides, indicating the contribution of alteration phases of the basaltic dust from different sources (Goetz et al., 2005; Madsen et al., 2009; Morris et al., 2006). This is also in agreement with the APXS analysis of air fall dust on the titanium observation tray of MSL that gave evidence of enrichments in S, Cl, and Fe consistent with previous studies (Berger et al., 2016).

Our new method to determine the eolian dust composition from the ChemCam's first shots strengthens the conclusions from previous studies. Dust composition measured in this way does present enrichments in the volatile elements S, Cl, and H, while increase in FeO and TiO_2 contents are probably linked to the presence of nanophase ferric oxides, such as titanomagnetite (Goetz et al., 2005). Overall, the major elements composition of the dust is similar to previous studies. The fact that eolian dust on opposite sides of the planet are similar is evidence of a frequent assumption, namely, that dust is a global product of the basaltic crust of Mars not

dominated by the composition of local rocks. On the other hand, it could also reflect the general similarity in compositions of the rocks from which they were derived. The latter hypothesis is unlikely, based on the presence of felsic and basaltic classes of grains in the local soils as discussed earlier.

4. Conclusions

In this work we have shown that every first shot taken by ChemCam contains information relevant to the composition of the eolian fine dust at Gale. A consistent chemical composition of the martian fine dust component can be retrieved by statistical analysis of the first shots taken on every target. The dust composition thus obtained remains significantly constant over the whole mission. The compositional homogeneity of the dust at the 350-micron scale of the ChemCam LIBS spot probably indicates an efficient mixing of the dust grains at this scale and/or the widespread presence of their lithic source.

The dust composition shows similar trends to the APXS dust measurements on the observation tray of MSL. There are significant differences with the Aeolis Palus soils and Bagnold dunes, as the dust is lower in CaO, and higher in SiO₂. The dust content in FeO and TiO₂ is larger than the soils and probably associated with nanophase oxides components, such as titanomagnetite. The dust spectra show the presence of volatile elements (S and Cl), and the hydrogen content is similar to Bagnold sands, but lower than Aeolis Palus soils. The dust may be a contributor to the amorphous component of soils, but differences in composition indicate that the two materials are not equivalent. This may be linked to the presence in the eolian dust of a mixture of altered and unaltered materials mixed over the planet in a global cycle. Therefore, dust may not constitute the most chemically altered soil component, and the physical weathering of unaltered phases of rocks and pebbles during their transport may have played an important role in its formation.

Acknowledgments

The authors acknowledge the constructive comments received from two anonymous referees and the Editor A. Dombard. The data used in this work can be found at NASA's Planetary Data System website as MSL-M-CHEMCAM-LIBS-4/5-RDR-V1.0. A .csv file containing all the first shots major oxide compositions used in the study with sequence numbers and targets' names is available as supporting information of the manuscript. This allows the reader to reproduce the main results presented (Table 1 and Figures 1, 2, and S5). The sequence of numbers and names also allows the reader to collect the correct spectra from the PDS repository. Support from the French Space Agency (CNES) and NASA's Mars Program Office is acknowledged.

References

- Achilles, C. N., Downs, R. T., Ming, D. W., Rampe, E. B., Morris, R. V., Treiman, A. H., et al. (2017). Mineralogy of an active eolian sediment from the Namib Dune, Gale Crater Mars. *Journal of Geophysical Research: Planets*, 122, 2344–2361. <https://doi.org/10.1002/2017JE005262>
- Arvidson, R. E., Gooding, J. L., & Moore, H. J. (1989). The martian surface as imaged, sampled, and analyzed by the viking landers. *Reviews of Geophysics*, 27(1), 39–60.
- Bandfield, J. L., Glotch, T. D., & Christensen, P. R. (2003). Spectroscopic identification of carbonate minerals in the martian dust. *Science*, 301(5636), 1084–1087.
- Beck, P., Fau, A., Meslin, P.-Y., Forni, O., Lasue, J., Lewin, E., et al. (2017). Searching for carbon on mars with MSL/ChemCam. In *Lunar and Planetary Science Conference* (Vol. 48, pp. 1216). The Woodlands, Texas
- Berger, J. A., King, P. L., Gellert, R., Campbell, J. L., Boyd, N. I., Pradler, I., et al. (2014). MSL-APXS titanium observation tray measurements: Laboratory experiments and results for the rocknest fines at the curiosity field site in Gale Crater, Mars. *Journal of Geophysical Research: Planets*, 119, 1046–1060. <https://doi.org/10.1002/2013JE004519>
- Berger, J. A., Schmidt, M. E., Gellert, R., Campbell, J. L., King, P. L., Flemming, R. L., et al. (2016). A global mars dust composition refined by the Alpha-Particle X-Ray Spectrometer in Gale Crater: Mars dust composition in Gale Crater. *Geophysical Research Letters*, 43, 67–75. <https://doi.org/10.1002/2015GL066675>
- Bish, D. L., Blake, D. F., Vaniman, D. T., Chipera, S. J., Morris, R. V., Ming, D. W., et al. (2013). X-ray diffraction results from Mars, Science Laboratory: Mineralogy of rocknest at Gale Crater. *Science*, 341(6153), 1238,932.
- Blake, D. F., Morris, R. V., Kocurek, G., Morrison, S. M., Downs, R. T., Bish, D., et al. (2013). Curiosity at Gale Crater, Mars: Characterization and analysis of the rocknest sand shadow. *Science*, 341(6153), 1239505. <https://doi.org/10.1126/science.1239505>
- Blake, D., Vaniman, D., Achilles, C., Anderson, R., Bish, D., Bristow, T., et al. (2012). Characterization and calibration of the chemin mineralogical instrument on Mars Science Laboratory. *Space Science Reviews*, 170(1-4), 341–399.
- Campbell, J. L., Perrett, G. M., Gellert, R., Andrushenko, S. M., Boyd, N. I., Maxwell, J. A., et al. (2012). Calibration of the Mars Science Laboratory Alpha Particle X-Ray Spectrometer. *Space Science Reviews*, 170(1-4), 319–340.
- Clancy, R. T., Lee, S. W., Gladstone, G. R., McMillan, W. W., & Rousch, T. (1995). A new model for mars atmospheric dust based upon analysis of ultraviolet through infrared observations from Mariner 9, Viking, and Phobos. *Journal of Geophysical Research*, 100(E3), 5251. <https://doi.org/10.1029/94JE01885>
- Clark, B. C., Baird, A. K., Weldon, R. J., Tsusaki, D. M., Schnabel, L., & Candelaria, M. P. (1982). Chemical composition of martian fines. *Journal of Geophysical Research*, 87(B12), 10,059–10,067.
- Clegg, S. M., Wiens, R. C., Anderson, R., Forni, O., Frydenvang, J., Lasue, J., et al. (2017). Recalibration of the Mars Science Laboratory ChemCam instrument with an expanded geochemical database. *Spectrochimica Acta Part B: Atomic Spectroscopy*, 129, 64–85. <https://doi.org/10.1016/j.sab.2016.12.003>
- Cousin, A., Dehouck, E., Meslin, P.-Y., Forni, O., Williams, A., Stein, N., et al. (2017). Geochemistry of the Bagnold dune field as observed by ChemCam and comparison with other aeolian deposits at Gale Crater. *Journal of Geophysical Research: Planets*, 122, 2144–2162. <https://doi.org/10.1002/2017JE005261>
- Cousin, A., Meslin, P. Y., Wiens, R. C., Rapin, W., Mangold, N., Fabre, C., et al. (2015). Compositions of coarse and fine particles in martian soils at Gale: A window into the production of soils. *Icarus*, 249, 22–42. <https://doi.org/10.1016/j.icarus.2014.04.052>
- Dehouck, E., McLennan, S. M., Meslin, P.-Y., & Cousin, A. (2014). Constraints on abundance, composition, and nature of x-ray amorphous components of soils and rocks at Gale Crater, Mars. *Journal of Geophysical Research: Planets*, 119, 2640–2657. <https://doi.org/10.1002/2014JE004716>
- Ehlmann, B. L., Edgett, K. S., Sutter, B., Achilles, C. N., Litvak, M. L., Lapotre, M. G., et al. (2017). Chemistry, mineralogy, and grain properties at Namib and high dunes, Bagnold dune field, Gale Crater Mars: A synthesis of curiosity rover observations. *Journal of Geophysical Research: Planets*, 122, 2510–2543. <https://doi.org/10.1002/2017JE005267>

- Fabre, C., Maurice, S., Cousin, A., Wiens, R. C., Forni, O., Sautter, V., & Guillaume, D. (2011). Onboard calibration igneous targets for the Mars Science Laboratory Curiosity Rover and the Chemistry Camera Laser Induced Breakdown Spectroscopy instrument. *Spectrochimica Acta Part B: Atomic Spectroscopy*, 66(3), 280–289. <https://doi.org/10.1016/j.sab.2011.03.012>
- Forni, O., Maurice, S., Gasnault, O., Wiens, R. C., Cousin, A., Clegg, S. M., et al. (2013). Independent component analysis classification of laser induced breakdown spectroscopy spectra. *Spectrochimica Acta Part B: Atomic Spectroscopy*, 86, 31–41.
- Gabriel, T. S. J., Hardgrove, C., Czarniecki, S., Rampe, W., Achilles, C. N., et al. (2018). Water abundance of dunes in Gale crater, Mars from active neutron experiments & implications for amorphous phases. *Geophysical Research Letters*, 45. <https://doi.org/10.1029/2018gl079045>
- Gellert, R., Rieder, R., Brückner, J., Clark, B. C., Dreibus, G., Klingelhöfer, G., et al. (2006). Alpha Particle X-Ray Spectrometer (APXS): Results from Gusev Crater and calibration report. *Journal of Geophysical Research*, 111, E02S05. <https://doi.org/10.1029/2005JE002555>
- Goetz, W., Bertelsen, P., Binau, C. S., Gunnlaugsson, H. P., Hviid, S. F., Kinch, K. M., et al. (2005). Indication of drier periods on Mars from the chemistry and mineralogy of atmospheric dust. *Nature*, 436(7047), 62.
- Gómez-Elvira, J., Armiens, C., Castañer, L., Domínguez, M., Genzer, M., Gómez, F., et al. (2012). REMS: The environmental sensor suite for the Mars Science Laboratory Rover. *Space Science Reviews*, 170(1–4), 583–640.
- Hamilton, V. E., McSween, H. Y., & Hapke, B. (2005). Mineralogy of martian atmospheric dust inferred from thermal infrared spectra of aerosols. *Journal of Geophysical Research*, 110, E12006. <https://doi.org/10.1029/2005JE002501>
- Johnson, J. R., Bell, J. F. III, Bender, S., Blaney, D., Cloutis, E., DeFlores, L., et al. (2015). ChemCam passive reflectance spectroscopy of surface materials at the Curiosity landing site, Mars. *Icarus*, 249, 74–92. <https://doi.org/10.1016/j.icarus.2014.02.028>
- Kleinböhl, A., Schofield, J. T., Kass, D. M., Abdou, W. A., Backus, C. R., Sen, B., et al. (2009). Mars Climate Sounder limb profile retrieval of atmospheric temperature, pressure, and dust and water ice opacity. *Journal of Geophysical Research*, 114, E10006. <https://doi.org/10.1029/2009JE003358>
- Klingelhofer, G., Morris, R. V., Bernhardt, B., Rodionov, D., de Souza, Jr. P. A., Squyres, S. W., et al. (2003). Athena MIMOS II Mössbauer spectrometer investigation. *Journal of Geophysical Research*, 108(E12), 8067. <https://doi.org/10.1029/2003JE002138>
- Lanza, N. L., Ollila, A. M., Cousin, A., Wiens, R. C., Clegg, S., Mangold, N., et al. (2015). Understanding the signature of rock coatings in Laser-Induced Breakdown Spectroscopy data. *Icarus*, 249, 62–73.
- Le Mouélic, S., Gasnault, O., Herkenhoff, K. E., Bridges, N. T., Langevin, Y., Mangold, N., et al. (2015). The ChemCam remote Micro-Imager at Gale Crater: Review of the first year of operations on Mars. *Icarus*, 249, 93–107. <https://doi.org/10.1016/j.icarus.2014.05.030>
- Lemmon, M. T., Wolff, M. J., Smith, M. D., Clancy, R. T., Banfield, D., Landis, G. A., et al. (2004). Atmospheric imaging results from the Mars exploration rovers: Spirit and opportunity. *Science*, 306(5702), 1753–1756. <https://doi.org/10.1126/science.1104474>
- Leshin, L. A., Mahaffy, P. R., Webster, C. R., Cabane, M., Coll, P., Conrad, P. G., et al. (2013). Volatile, isotope, and organic analysis of martian fines with the Mars Curiosity rover. *Science*, 341(6153), 1238937. <https://doi.org/10.1126/science.1238937>
- Madsen, M. B., Bertelsen, P., Goetz, W., Binau, C. S., Olsen, M., Folkmann, F., et al. (2003). Magnetic properties experiments on the Mars Exploration Rover Mission. *Journal of Geophysical Research*, 108(E12), 8069. <https://doi.org/10.1029/2002JE002029>
- Madsen, M. B., Goetz, W., Bertelsen, P., Binau, C. S., Folkmann, F., Gunnlaugsson, H. P., et al. (2009). Overview of the magnetic properties experiments on the Mars Exploration Rovers. *Journal of Geophysical Research*, 114, E06S90. <https://doi.org/10.1029/2008JE003098>
- Maurice, S., Wiens, R. C., Saccoccio, M., Barraclough, B., Gasnault, O., Forni, O., et al. (2012). The ChemCam instrument suite on the Mars Science Laboratory (MSL) Rover: Science objectives and mast unit description. *Space Science Reviews*, 170, 95–166. <https://doi.org/10.1007/s11214-012-9912-2>
- McCleese, D. J., Schofield, J. T., Taylor, F. W., Calcutt, S. B., Foote, M. C., Kass, D. M., et al. (2007). Mars Climate Sounder: An investigation of thermal and water vapor structure, dust and condensate distributions in the atmosphere, and energy balance of the polar regions. *Journal of Geophysical Research*, 112, E05S06. <https://doi.org/10.1029/2006JE002790>
- Melikechi, N., Mezzacappa, A., Cousin, A., Lanza, N. L., Lasue, J., Clegg, S. M., et al. (2014). Correcting for variable laser-target distances of laser-induced breakdown spectroscopy measurements with ChemCam using emission lines of Martian dust spectra. *Spectrochimica Acta Part B: Atomic Spectroscopy*, 96, 51–60. <https://doi.org/10.1016/j.sab.2014.04.004>
- Meslin, P.-Y., Ganault, O., Forni, O., Schröder, S., Cousin, A., Berger, G., et al. (2013). Soil diversity and hydration as observed by ChemCam at Gale Crater, Mars. *Science*, 341(6153), 1238670. <https://doi.org/10.1126/science.1238670>
- Mezzacappa, A., Melikechi, N., Cousin, A., Wiens, R. C., Lasue, J., Clegg, S. M., et al. (2016). Application of distance correction to ChemCam Laser-Induced Breakdown Spectroscopy measurements. *Spectrochimica Acta Part B: Atomic Spectroscopy*, 120, 19–29. <https://doi.org/10.1016/j.sab.2016.03.009>
- Ming, D. W., Gellert, R., Morris, R. V., Arvidson, R. E., Brueckner, J., Clark, B. C., et al. (2008). Geochemical properties of rocks and soils in Gusev Crater, Mars: Results of the Alpha Particle X-Ray Spectrometer from Cumberland Ridge to Home Plate. *Journal of Geophysical Research*, 113, E12S39. <https://doi.org/10.1029/2008JE003195>
- Montmessin, F. (2002). New insights into martian dust distribution and water-ice cloud microphysics. *Journal of Geophysical Research*, 107(E6), 5037. <https://doi.org/10.1029/2001JE001520>
- Morris, R. V., Klingelhofer, G., Schröder, C., Rodionov, D. S., Yen, A., Ming, D. W., et al. (2006). Mössbauer mineralogy of rock, soil, and dust at Gusev Crater, Mars: Spirit's journey through weakly altered olivine basalt on the plains and pervasively altered basalt in the Columbia Hills. *Journal of Geophysical Research*, 111, E02S13. <https://doi.org/10.1029/2005JE002584>
- O'Connell-Cooper, C. D., Spray, J. G., Thompson, L. M., Gellert, R., Berger, J. A., Boyd, N. I., et al. (2017). APXS-derived chemistry of the Bagnold dune sands: Comparisons with Gale Crater soils and the global martian average. *Journal of Geophysical Research: Planets*, 122, 2623–2643. <https://doi.org/10.1002/2017JE005268>
- Ojha, L., Lewis, K., Karunatillake, S., & Schmidt, M. (2018). The Medusae Fossae Formation as the single largest source of dust on Mars. *Nature Communications*, 9(1), 2867. <https://doi.org/10.1038/s41467-018-05291-5>
- Ollila, A. M., Blank, J. G., Wiens, R. C., Lasue, J., Newsom, H. E., Clegg, S. M., et al. (2011). Preliminary results on the capabilities of the ChemCam, Laser-Induced Breakdown Spectroscopy (LIBS) instrument to detect carbon on Mars. In *Lunar and Planetary Science Conference* (Vol. 42, pp. 2395). The Woodlands, TX.
- Ollila, A. M., Newsom, H. E., Wiens, R. C., Lasue, J., Clegg, S. M., Cousin, A., et al. (2013). Early results from Gale, Crater on ChemCam detections of carbon, lithium, and rubidium. In *Lunar and Planetary Science Conference* (Vol. 44, pp. 2188). USA.
- Pollack, J. B., Ockert-Bell, M. E., & Shepard, M. K. (1995). Viking lander image analysis of martian atmospheric dust. *Journal of Geophysical Research*, 100(E3), 5235. <https://doi.org/10.1029/94JE02640>
- Rapin, W., Meslin, P.-Y., Maurice, S., Wiens, R. C., Laporte, D., Chauviré, B., et al. (2017). Quantification of water content by Laser Induced Breakdown Spectroscopy on Mars. *Spectrochimica Acta Part B: Atomic Spectroscopy*, 130, 82–100.
- Rieder, R., Gellert, R., Brückner, J., Klingelhöfer, G., Dreibus, G., Yen, A., & Squyres, S. W. (2003). The new Athena Alpha Particle X-Ray Spectrometer for the Mars Exploration Rovers. *Journal of Geophysical Research*, 108(E12), 8066. <https://doi.org/10.1029/2003JE002150>
- Ruff, S. W. (2004). Spectral evidence for zeolite in the dust on Mars. *Icarus*, 168(1), 131–143.

- Sautter, V., Fabre, C., Forni, O., Toplis, M. J., Cousin, A., Ollila, A. M., et al. (2014). Igneous mineralogy at Bradbury Rise: The first ChemCam campaign at Gale Crater. *Journal of Geophysical Research: Planets*, *119*, 30–46. <https://doi.org/10.1002/2013JE004472>
- Schröder, S., Meslin, P.-Y., Gasnault, O., Maurice, S., Cousin, A., Wiens, R. C., et al. (2015). Hydrogen detection with ChemCam at Gale Crater. *Icarus*, *249*, 43–61. <https://doi.org/10.1016/j.icarus.2014.08.029>
- Stolper, E. M., Baker, M. B., Newcombe, M. E., Schmidt, M. E., Treiman, A. H., Cousin, A., et al. (2013). The petrochemistry of Jake_m: A martian mugearite. *Science*, *341*(6153), 1239463.
- Sutter, B., Mcadam, A. C., Mahaffy, P. R., Ming, D. W., Edgett, K. S., Rampe, E. B., et al. (2017). Evolved gas analyses of sedimentary rocks and eolian sediment in Gale Crater, Mars: Results of the Curiosity Rover's sample analysis at Mars instrument from Yellowknife Bay to the Namib Dune. *Journal of Geophysical Research: Planets*, *122*, 2574–2609. <https://doi.org/10.1002/2016JE005225>
- Taylor, S. R., & McLennan, S. (2009). *Planetary crusts: Their composition, origin and evolution*. New York: Cambridge University Press.
- Tomasko, M. G., Doose, L. R., Lemmon, M., Smith, P. H., & Wegryn, E. (1999). Properties of dust in the martian atmosphere from the imager on Mars Pathfinder. *Journal of Geophysical Research*, *104*(E4), 8987–9007. <https://doi.org/10.1029/1998JE900016>
- Toon, O. B., Pollack, J. B., & Sagan, C. (1977). Physical properties of the particles composing the martian dust storm of 1971-1972. *Icarus*, *30*(4), 663–696. [https://doi.org/10.1016/0019-1035\(77\)90088-4](https://doi.org/10.1016/0019-1035(77)90088-4)
- Vaniman, D., Dyar, M. D., Wiens, R., Ollila, A., Lanza, N., Lasue, J., et al. (2012). Ceramic ChemCam calibration targets on Mars Science Laboratory. *Space Science Reviews*, *170*, 229–255. <https://doi.org/10.1007/s11214-012-9886-0>
- Vaughan, A. F., Johnson, J. R., Herkenhoff, K. E., Sullivan, R., Landis, G. A., Goetz, W., & Madsen, M. B. (2010). Pancam and microscopic imager observations of dust on the Spirit rover: Cleaning events, spectral properties, and aggregates, Mars. *The International Journal of Mars Science and Exploration*, *5*, 129–145.
- Vincendon, M., Langevin, Y., Poulet, F., Pommerol, A., Wolff, M., Bibring, J. P., et al. (2009). Yearly and seasonal variations of low albedo surfaces on Mars in the OMEGA/MEx dataset: Constraints on aerosols properties and dust deposits. *Icarus*, *200*(2), 395–405. <https://doi.org/10.1016/j.icarus.2008.12.012>
- Wiens, R. C., Maurice, S., Barraclough, B., Saccoccio, M., Barkley, W. C., Bell, J. F. III., et al. (2012). The ChemCam instrument suite on the Mars Science Laboratory (MSL) rover: Body unit and combined system tests. *Space Science Reviews*, *170*(1-4), 167–227. <https://doi.org/10.1007/s11214-012-9902-4>
- Wiens, R. C., Maurice, S., Lasue, J., Forni, O., Anderson, R. B., Clegg, S., et al. (2013). Pre-flight calibration and initial data processing for the ChemCam Laser-Induced Breakdown Spectroscopy instrument on the Mars Science Laboratory rover. *Spectrochimica Acta Part B: Atomic Spectroscopy*, *82*, 1–27. <https://doi.org/10.1016/j.sab.2013.02.003>
- Wolff, M. J., Smith, M. D., Clancy, R. T., Spanovich, N., Whitney, B. A., Lemmon, M. T., et al. (2006). Constraints on dust aerosols from the Mars Exploration Rovers using MGS overflights and mini-TES. *Journal of Geophysical Research*, *111*, E12S17. <https://doi.org/10.1029/2006JE002786>
- Yen, A. S., Gellert, R., Schröder, C., Morris, R. V., Bell, J. F. III, Knudson, A. T., et al. (2005). An integrated view of the chemistry and mineralogy of martian soils. *Nature*, *436*(7047), 49–54. <https://doi.org/10.1038/nature03637>